VOL. 17, NO. 11, NOVEMBER 1979 AIAA JOURNAL 1243

ARTICLE NO. 79-0016R

Turbulence Effects on Flame Speed and Flame Structure

K. O. Smith* and F. C. Gouldin†
Cornell University, Ithaca, N.Y.

Turbulence effects on methane-air flames stabilized in grid turbulence were investigated through measurements of flame speed and mean and fluctuating flame temperature profiles. Published turbulent flame speed correlations were able to correlate the experimental flame speed data but were contradictory in indicating flame structure and combustion mechanisms. A simple, one-dimensional, wrinkled laminar flame model was used to predict characteristic flame temperature fluctuation levels. Comparison of these predictions with measured temperature fluctuations indicated that the majority of the flames studied were wrinkled laminar flames. However, a wrinkled laminar flame structure was inappropriate for the most intensely turbulent flames examined.

Introduction

In a previous paper, a novel flame speed measurement technique for stationary turbulent flames was presented.[1] This technique represents an improvement over more commonly employed flame speed measurement techniques because of the local nature of the measurements. Flame speed is determined locally on the flame surface using fine-wire thermocouples to determine the flame surface orientation and hot-film and laser anemometry for velocity and turbulence measurements. The flame speed measurement technique can provide more reliable experimental data and should be more valuable in assessing proposed turbulent flame speed correlations.

In this paper, experimental flame speed data obtained with the improved measurement technique are used to assess a number of turbulent flame speed correlations found in the literature. In addition, the uncertainty in attempting to infer flame structure from flame speed correlations is demonstrated. Finally, root mean square (rms) flame temperature fluctuation measurements obtained by modifying the flame speed measurement instrumentation are presented. The temperature fluctuations data are used to determine whether a wrinkled laminar flame structure is consistent with the observed flame characteristics.

Experimental Apparatus

Unconfined, methane-air flames were investigated in this study. Flames that appeared V-shaped in profile were obtained by mounting a cylindrical flameholder (1.25-mm diam) across the exit of a cylindrical burner (5.08-cm diam). Screens upstream of the flameholder were used to produce turbulence of varying intensity ($I=u'/U$) and macroscale (ℓ). u' and U represent, respectively, the rms velocity fluctuation and mean velocity parallel to the combustor axis. Two wire-woven screens (no. 10 and no. 20 mesh) and a perforated plate (grid generator) were employed as turbulence generators. The apparatus provided turbulent flows of up to 7% intensity with exit velocities up to 30 m/s. Macroscales ranged from 0.6 to 1.66 mm. Equivalence ratio (ϕ) was varied from 0.75 to 1.00.

Presented as Paper 79-0016 at the AIAA 17th Aerospace Sciences Meeting, New Orleans, La., Jan. 15-17, 1979; submitted Feb. 26, 1979; revision received May 29, 1979.

Index categories: Combustion and Combustor Designs; Fuels and Propellants, Properties of.

*Graduate Research Assistant, Sibley School of Mechanical and Aerospace Engineering. Currently at Solar Turbines International, San Diego, Calif.

†Associate Professor, Sibley School of Mechanical and Aerospace Engineering.

Instrumentation and Measurement Technique

Figure 1 illustrates the flame speed measurement technique adopted for this study. 0.127-mm (5-mil) Pt/Pt10Rh thermocouples were used to establish the local, time mean flame front inclination relative to the combustor axis. The flame front was defined by the $2T_0$ isotherm, following the recommendation that flame speed be determined at the surface of initial gas temperature increase.[2] T_0 represents the temperature of the unburned fuel and air mixture. A hot-film anemometer (TSI 1050) was used to measure mean velocity magnitudes. A laser anemometer system incorporating a tracking signal processor (Disa 55L) was used to determine the mean-flow direction relative to the combustor axis. Flame speed was taken as equal in magnitude to the approach flow velocity component normal to the time mean position of the flame front.

Flame speed measurements were conducted at a fixed location downstream of the turbulence generating screens (h) and the flame stabilizer. At a fixed distance downstream of any single turbulence generator, I and ℓ remained essentially constant over the range of combustor velocities investigated. This permitted u' and ℓ, as well as ϕ, to be varied independently.

Flow turbulence characteristics corresponding to the turbulent flame speed data were measured using hot-film anemometry. Measurements of I, ℓ, and microscale (λ) were conducted at the same location as the flame speed measurement but in noncombusting flows.

The flame speed measurement instrumentation was also used in a modified form to measure the rms flame temperature fluctuation profiles of a number of flames. The amplified signals of 0.076-mm (3-mil), Pt/Pt10Rh, silica-coated thermocouples were electronically compensated (TSI 1015C) for the thermal inertia of the temperature sensors. Thermocouple time constants were determined by the method of Ref. 3 where the thermocouple response to a simulated step change in gas temperature was evaluated. Compensation extended the thermocouple response from about 3 Hz to approximately 400 Hz. More complete descriptions of all of the instrumentation and measurement techniques utilized in this study can be found in Refs. 1 and 4.

Summary of Flame Speed Measurements

Figure 2 illustrates the flame speed data obtained with the no. 10 mesh turbulence generator. These data are typical of all of the flame speed data obtained in this study which were previously reported.[1,4] Turbulent flame speed (S_t) increases

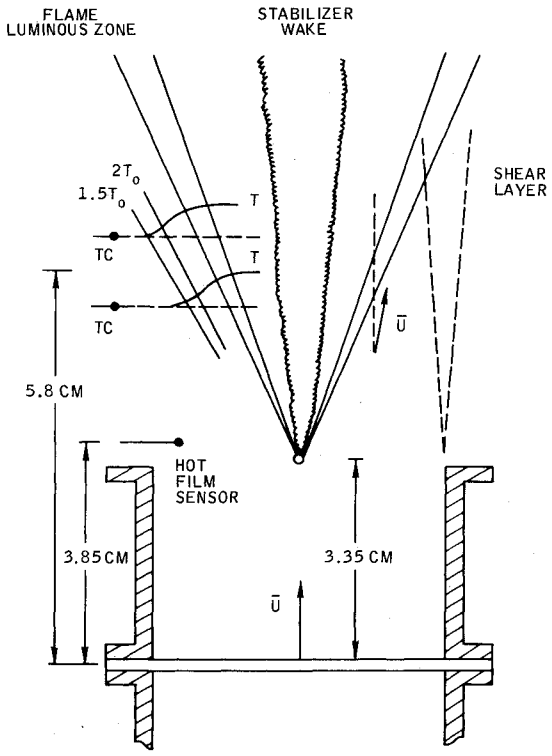

Fig. 1 Combustion section of experimental apparatus and flame speed measurement configuration.

with increased u' and ϕ. S_t also increases with increased ℓ at fixed u' and ϕ. Finally, all of the data show two regimes of flame speed behavior. At fixed ℓ and ϕ and low combustor velocities, flame speed increases with increased u' but with a decreasing rate. At higher velocities S_t appears linearly related to u'. This high-velocity regime is due to the flames stabilizing in the flameholder wake. This paper is concerned only with the flame speed data corresponding to the low combustor velocity regime where the flames are influenced primarily by the approach flow turbulence. The flame speed data from flames in the flameholder wake are not considered because of the uncertainty in defining a characteristic turbulence intensity and macroscale that dominate the combustion processes.

Overview of Turbulent Flame Structure

A majority of the mechanistic turbulent flame structure models found in the literature can be classified into three groups.[5] These three distinct types are the wrinkled laminar flame (WLF) and combusting eddy models with either the large- or small-scale turbulent structure assuming a dominant role in the combustion process.

In low-intensity turbulence, it is generally accepted that turbulence acts primarily to wrinkle the continuous flame sheet associated with laminar combustion.[6] The wrinkled flame maintains its continuous nature. Locally, the flame sheet propagates normal to itself at essentially the laminar flame speed.[5] However, increased apparent flame speeds result from increased flame surface areas. In the limit of extremely low turbulence intensity, the local combustion zone structure may be essentially identical to a laminar combustion zone.[6]

Although long-exposure photographs of a WLF indicate a thick luminous flame brush, instantaneously, chemical reaction is limited to a thin combustion zone within the thicker flame brush. The indicated flame brush thickness is attributable to the fluctuating combustion zone. Most frequently, the existence of a WLF structure is suggested by schlieren photographs that show surfaces with large-scale wrinkles or swellings but still maintaining an overall smooth

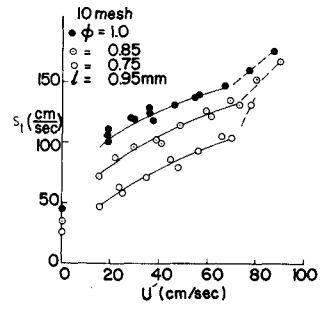

Fig. 2 Variation of turbulent flame speed with rms fluctuating velocity.

laminar appearance.[7]

Increased turbulence intensities tend to disrupt the continous nature of the flame sheet associated with the WLF. Combustion may be pictured mechanistically as occurring in a region characterized by an ensemble of discrete flame segments or flamelets. The local structure of these flamelets may show significant deviations from a laminar flame due to local turbulence flame stretch effects.[8] Combustion in this regime may be conceptualized as resulting from flamelets that separate regions of burned and unburned gases, or, perhaps, as turbulent eddies of unburned gases that are undergoing a surface combustion process.

For flames in high-intensity turbulence, the small-scale structure of the turbulence dominates combustion. Combustion in this highly turbulent regime may no longer be limited to thin combustion zones. Instead, as postulated by Summerfield, reactions may occur, instantaneously, across the entire thickness of the time-averaged combustion region.[9] Alternative mechanisms have been postulated by Schetinkov[10] as the volumetric combustion of turbulent eddies and by Chomiak[11] as combustion limited to intermittent regions associated with intense turbulent mixing. In these proposed mechanisms small-scale mixing assumes an important role. Schlieren photographs of flames in intensely turbulent flows indicate a highly distorted and roughened flame surface in contrast to the WLF. Combustion does not appear to be limited to a relatively thin, well-defined, continuous reaction zone.[7]

Conditions for a WLF

A number of parameters have been proposed in an effort to distinguish between proposed combustion regimes. Both Kovasnay[12] and Klimov[8] employed the parameter Γ to predict the conditions in which a WLF would exist. Γ is defined as

$$\Gamma = \delta_L u'/S_L \lambda$$

δ_L and S_L are the laminar flame thickness and flame speed, respectively. Kovasnay reasoned that a WLF would exist when flow velocity gradients were much less than flame velocity gradients, $\Gamma \ll 1$. Klimov derived essentially the same parameter through an analysis of the conservation equations of a laminar flame in a shear flow. For the present study, values of Γ range from 0.03 to 0.4. The bulk of the data satisfy relatively well the criterion $\Gamma \ll 1$, which indicates that combustion occurs in a laminar flame mode.

Based on their experimental flame speed data, Ballal and Lefebvre proposed a three-regime classification of turbulent combustion processes.[7] The parameters u'/S_L and η/S_L were used to distinguish the three regimes. η represents the Kolomogorov microscale of the turbulence. The flames investigated in this study generally satisfy the criteria $u'/S_L < 2$ and $\eta/S_L > 1$, which indicate a WLF regime. η was estimated using the relationship[13]:

$$\eta/\lambda = 15^{-1/4} (u'\lambda/\nu)^{-1/2}$$

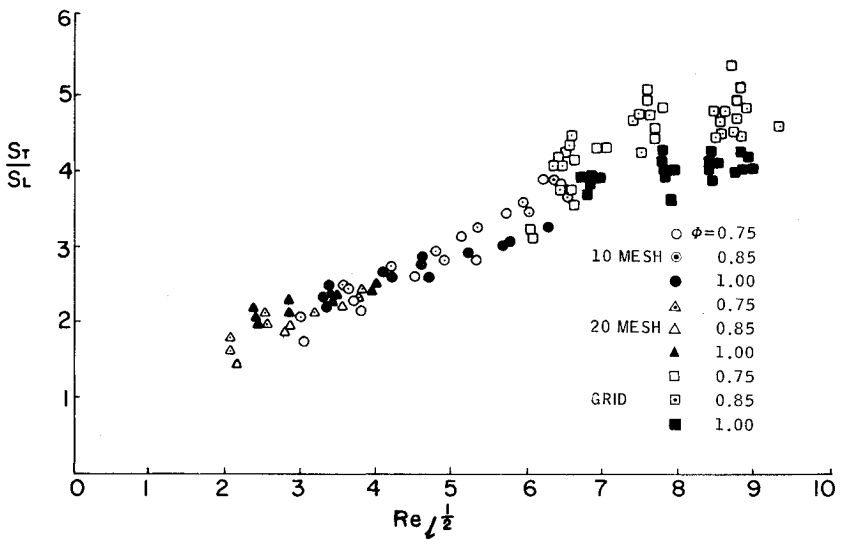

Fig. 3 Turbulent flame speed correlation: S_t/S_L vs $Re_\ell^{1/2}$.

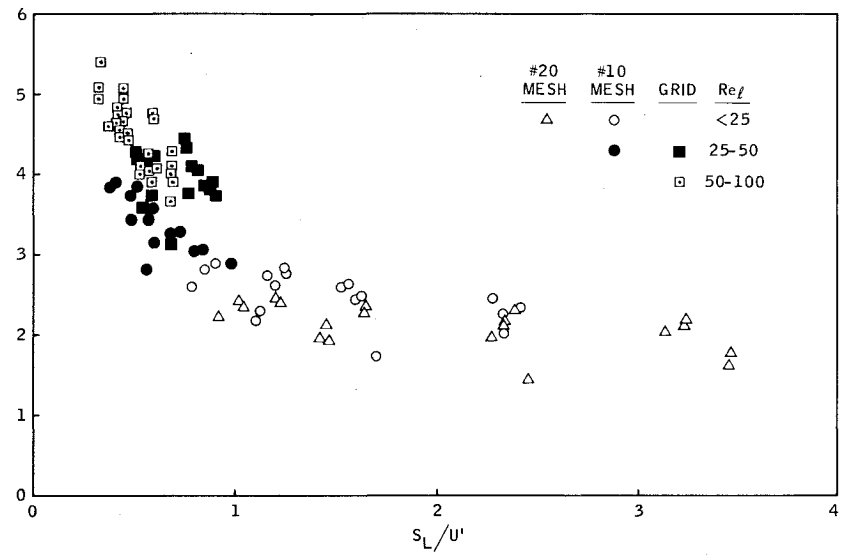

Fig. 4 Turbulent flame speed correlation: S_t/S_L vs S_L/u' and Re_ℓ.

However, some of the flames violate these criteria, which suggests that these flames correspond to more intensely turbulent combustion regimes.

Andrews et al.[14] discussed the importance of small-scale mixing in intensely turbulent flames. They argued that for values of the microscale Reynolds number Re_λ greater than 100, turbulent flows were characterized by a significant separation in size of the large- and small-scale structure of the turbulence. Since WLF models assume only large-scale wrinkling of the flame with no small-scale effects, Andrews et al. reasoned that the WLF regime was compatible with the criterion $Re_\lambda < 100$. The present study was limited to turbulent flames characterized by $Re_\lambda < 40$.

Gouldin defined intensely turbulent flames using the criterion $u'/S_L > 1$.[15] In this condition, the eddy breakup time, ℓ/u', is shorter than the time scale for the consumption of an eddy by a laminar flame, ℓ/S_L. For $u'/S_L > 1$, a continuous flame sheet can no longer exist. The present study has achieved a maximum value of u'/S_L of approximately 3. By this criterion, some of the more turbulent flames may reflect combustion controlled by turbulence dynamics rather than a laminar combustion mode.

The parameters just discussed indicate that a majority of the flames investigated in this study should be characterized by a WLF mode of combustion. Some of the more turbulent flames, however, may reflect combustion in a regime more characteristic of practical combustion devices. It should be realized of course that, with the possible exception of Klimov's work, the preceding parameters are based largely on heuristic arguments. The validity of these parameters has never been tested rigorously. Further, it is clear that these parameters were not intended to represent precise transition points between turbulent combustion regimes. Rather, they suggest the general conditions in which a turbulent flame is no longer described accurately in terms of laminar combustion processes.

Turbulent Flame Speed Correlations

A number of previous workers have attempted to correlate experimental flame speed data from flames in low-intensity turbulence using a turbulent diffusivity correlating parameter ($u'\ell$) to represent turbulence effects. In this WLF regime,. u' and ℓ are described as acting to increase the flame surface area by wrinkling. The larger flame area results in larger reactant consumption rates as reflected by increased turbulent flame speeds. However, differences do exist in the various adopted correlating parameters and their functional relationships.

Sanematsu correlated his low-intensity flame speed data ($I < 3\%$) with the parameters S_t/S_L and $u'\ell/S_L b$, where b is a characteristic length of the turbulence generators.[16] The appearance of b in the correlation implies that flame speed is combustor dependent. Sanematsu found that the correlating parameters were linearly related and adequately represented changes in both ϕ and turbulence properties. His attempts to

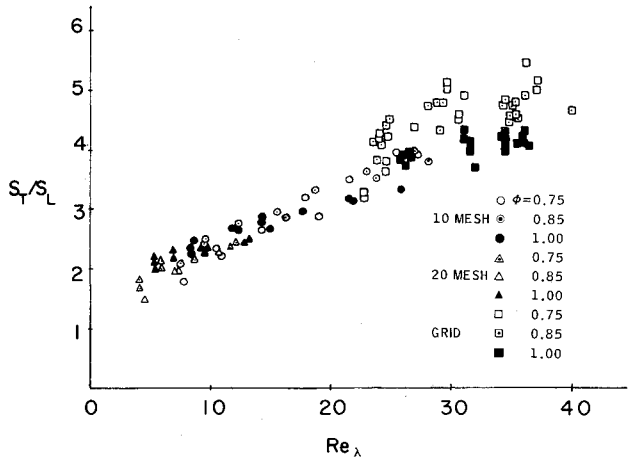

Fig. 5 Turbulent flame speed correlation: S_t/S_L vs Re_λ.

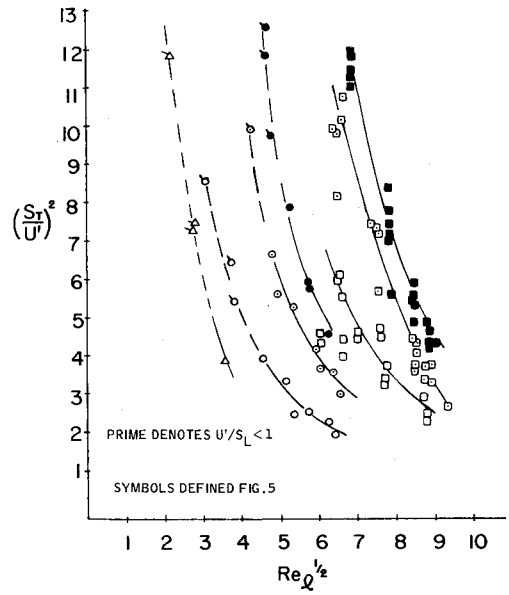

Fig. 6 Turbulent flame speed correlation: $(S_t/u')^2$ vs $Re_\ell^{1/2}$.

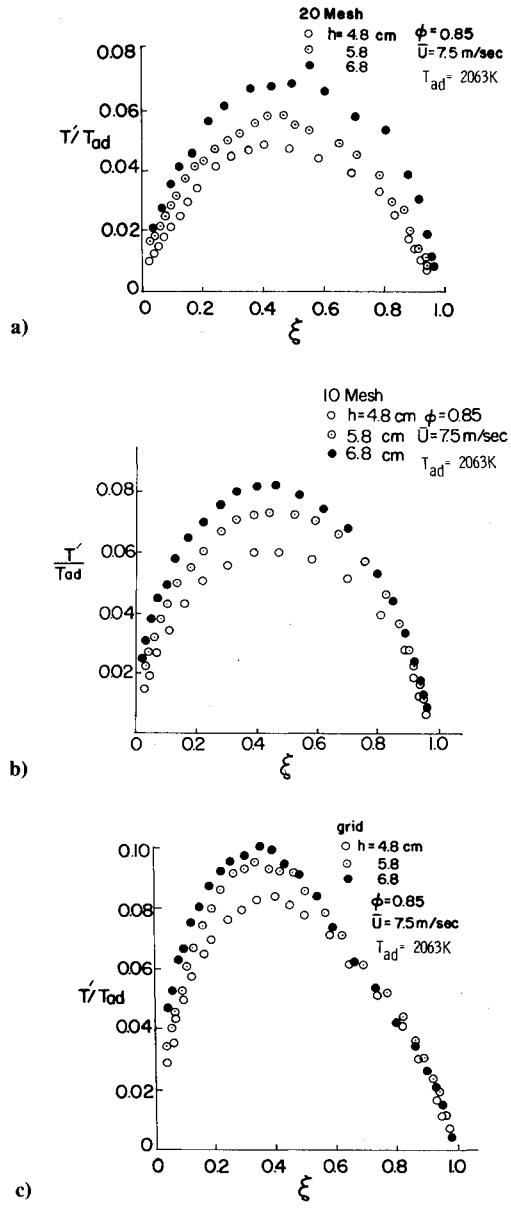

Fig. 7 rms temperature fluctuation profile.

correlate the experimental data of other workers were less successful. In addition, the flame speed data from the present study do not substantiate the S_t/S_L vs $u'\ell/S_L b$ correlation.

Wagner proposed an S_t/S_L vs Re_ℓ correlation without any statement as to the mechanisms controlling combustion.[17] Re_ℓ is the turbulence Reynolds number based on macroscale, $u'\ell/\nu$. Ballal and Lefebvre suggested a similar correlation of S_t/S_L vs $u'\ell/S_L\delta_L$ based on their experimental flame speed data for flames assumed to represent a WLF structure.[7] Assuming unit Prandtl number, a simplified laminar flame analysis shows[18]:

$$\delta_L \propto \nu/S_L$$

Therefore,

$$u'\ell/S_L\delta_L \propto Re_\ell$$

Ballal and Lefebvre reported a correlation of the form

$$S_t/S_L = \{1 + C_1(u'\ell/S_L\delta_L)^2\}^{1/2}$$

where C_1 is a constant.

Figure 3 presents an S_t/S_l vs Re_ℓ correlation of the flame speed data from the present study for flames in grid turbulence. The correlation reflects the increase in S_t resulting from increase in u', ℓ, and ϕ. The data suggest a relationship of the form

$$S_t/S_L = C_1 + C_2 Re_\ell^{1/2}$$

More extensive testing, particularly with different fuels, is required to establish the general validity of this relationship.

Evident in Fig. 3 is the inability of the experimental apparatus to provide extensively overlapping S_t data with the three turbulence generators employed. Instead, S_t data collected with a single generator tend to fall in a range of Re_ℓ that overlaps only slightly with the range achievable with the other turbulence generators. The data corresponding to higher values of Re_ℓ exhibit more scatter than the other data and were obtained with the grid generator. It may be argued that the larger scatter of these data indicates that the S_t/S_L vs Re_ℓ correlation is more appropriate for flames where $Re_\ell < 50$. However, data beyond the range of the present apparatus would have to be obtained to document this conclusion. Such an argument would be consistent with current concepts regarding flame structure. The flames downstream of the grid generator most significantly violate various criteria proposed to indicate the WLF regime. Since abrupt transitions in turbulent flame structure are unlikely with only slight changes

in turbulence properties, the inability of parameters to correlate flame speed data beyond a certain regime may develop only slowly.

Abel-Gayed and Bradley discussed a flame speed correlation of the form[19]

$$S_t/S_L = f(S_L/u', \quad Re_\ell)$$

using flame speed data from the literature and their own measurements. Data over a large range of operating conditions, Re_ℓ to 2000, were used to show that S_t/S_L decreased with increasing S_L/u' and decreasing Re_ℓ. The correlation was presented as valid over the spectrum of postulated flame structure regimes from the WLF to highly turbulent flames. No general theoretical expression for the correlation was suggested.

Figure 4 shows the data from this study plotted following Ref. 19 and employing the authors' ranges for the parameter Re_ℓ. A definitive assessment of the proposed correlation was not possible. The dependence of S_t/S_L on both S_L/u' and Re_t could not be established because of insufficient overlapping of the flame speed data with the turbulence generators employed. However, for $Re_\ell < 25$, where the WLF structure is most appropriate, it appears that the parameters S_t/S_L and Re_ℓ correlate the flame speed data with less scatter than the correlation of S_t/S_L vs Re_ℓ and S_L/u'.

The success of the S_t/S_L and $Re_\ell^{1/2}$ correlation is in qualitative agreement with previous investigations in that low-intensity turbulent flame speed data are correlated using parameters incorporating the turbulent diffusivity and laminar flame speed. However, the diffusivity itself does not suggest a specific mechanism through which turbulence increases flame speed. The correlation does not substantiate a WLF structure. For example, Summerfield's distributed reaction zone model predicts[9]:

$$S_t/S_L \propto u'\ell\delta_L/\nu\delta_t$$

Reference 20 predicts that for intensely turbulent flames:

$$(S_t/u')^2 = f(\sqrt{u'\ell/\nu})$$

The diffusivity which is characterized as causing flame wrinkling in low-intensity turbulence is associated with different combustion mechanisms in highly turbulent flames. Because of this, experimental flame speed data frequently satisfy correlations proposed for both the WLF regime and more intensely turbulent flames.

Andrews et al. suggested an S_t/S_L vs Re_λ correlation for intensely turbulent flames, $Re_\lambda > 100$. Figure 5 presents the data of this study correlated using these parameters. Although the experimental results do not exceed a Re_λ of 40, the Re_λ correlation appears to be as successful as the Re_ℓ correlation. The explanation for this ambiguity lies in the relatively small separation of ℓ and λ for the turbulent flows employed in this study. While either Re_λ or Re_ℓ may correlate flame speed data from flames in low-intensity turbulence, in more intense turbulence where macroscale and microscale magnitudes are significantly different, the Re_λ parameter may be preferable. Figure 5 suggests a linear relationship between S_t/S_L and Re_λ. This is in accord with Fig. 3 which indicated $S_t/S_L \propto Re_\ell^{1/2}$ since $Re_\ell^{1/2} \propto Re_\lambda$.

Gouldin states that a WLF does not exit for $u'/S_L \geq 1$.[15] Rather, turbulence dynamic controls the combustion of large turbulent eddies. For these intensely turbulent flames: $(S_t/u')^2 \propto Re_\ell^{1/2}$. This correlation of the present flame speed data is shown in Fig. 6. Data for u'/S_L both greater and less than unity have been included. The latter points are included to illustrate the lack of a sharp transition in flame speed behavior with the parameter u'/S_L. This underscores the idea that transitions in flame structure and propagation mechanisms are gradual in nature.

Figure 6 exhibits considerable scatter, particularly for the grid data. It is clear, however, that constants employed in the derivation of the flame speed correlation must differ significantly with changes in ϕ and turbulence properties. For this correlation to be generally valid, it will be necessary to quantify the relationships between the empirical constants employed and the existing chemical and turbulence characteristics. It is not possible on the basis of these data to determine whether $(S_t/u')^2$ is linearly related to $Re_\ell^{1/2}$ as suggested by experimental data obtained from more highly turbulent flames.[15] It should be recognized that the present data barely satisfy the proposed criterion for intensely turbulent flames. A more definitive evaluation of the correlation requires data from significantly more turbulent flames.

The flame speed data obtained in this study are correlated relatively well by a number of parameters. Correlations involving

$$S_t/S_L \propto Re_\ell^{1/2} \quad \text{or} \quad (u'\ell/S_L\delta_L)^{1/2}$$

and

$$S_t/S_L \propto Re_\lambda$$

do an adequate job in correlating the present data. The correlation of $(S_t/u')^2$ vs $Re_\ell^{1/2}$ may prove equally successful if the employed empirical factors can be related to flow and chemical characteristics. It should be noted that variations of the first set of correlating parameters have generally been associated with flames in low-intensity turbulence where a WLF structure is expected. The latter two correlations are associated with intensely turbulent flames and should be inappropriate for wrinkled flames. Clearly, parameters such as Re_λ, Re_ℓ, u'/S_L, and η/δ_L can be used to indicate general trends in flame speed behavior. However, these simple correlations are not capable of indicating unambiguously turbulent flame structure and combustion mechanisms.

Temperature Fluctuation Measurements

To investigate flame structure more directly, mean and fluctuating flame temperature measurements were conducted using electronically compensated thermocouples. Measurements were conducted at a relatively low combustor exit velocity, 7.5 m/s to minimize the turbulence kinetic energy beyond the 400-Hz frequency limit of the sensor. However, typical turbulence energy spectra indicated significant kinetic energy at 1000 Hz even for low exit velocities. Therefore, it is likely that temperature fluctuations occurred at frequencies beyond the flat response of the thermocouples.

Root mean square temperature fluctuations measurements (T') were conducted for various approach flow turbulence intensities and equivalence ratios. T' profiles were measured at various heights in the flames. Typical results are presented in Fig. 7. T' profiles are presented for flames above each of the three turbulence generators with $\phi = 0.85$. T', normalized using the adiabatic flame temperature (T_{ad}), is presented as function of the local mean flame temperature ($\bar{T}$), normalized as

$$\xi = (\bar{T} - T_0)/(T_{ad} - T_0)$$

For any single flame, T' increases with increased height in the flame. In addition, T' increases with increased ϕ and with increasingly coarse turbulence generators. Apparently flame structure and flame propagation effects as well as turbulence influence T' levels are reflected by the influence of ϕ. The increases in T' with ϕ are larger than can be attributed solely to associated flame temperature increases with ϕ. All of the flames investigated show peak T' levels near the central portion of the ξ profiles. However, flames in the grid-generated turbulence exhibit a definite shift in the T' peak to

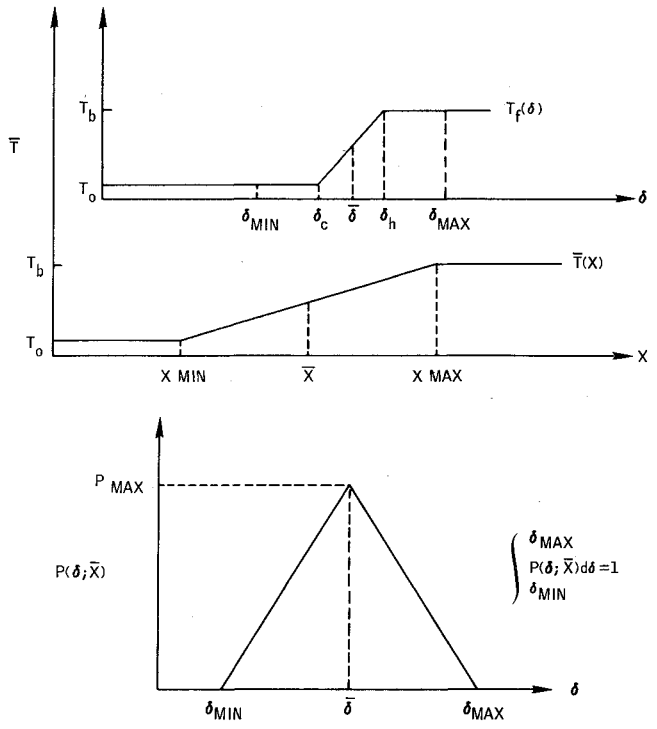

Fig. 8 Terminology for turbulent flame structure model.

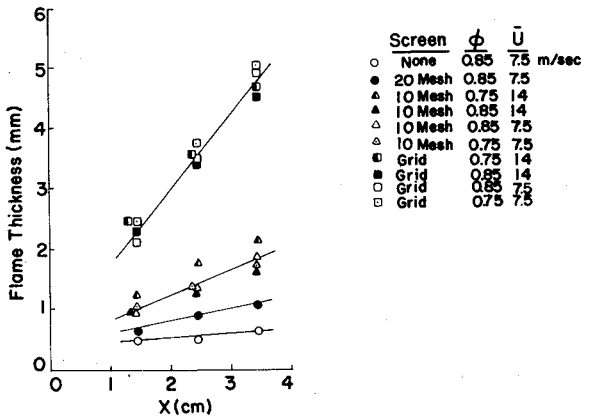

Fig. 9 Variation of flame thickness with distance from flameholder.

lower values of ξ relative to the flames above the less turbulent no. 10 and no. 20 mesh flows.

Wrinkled Laminar Flame Model

As already shown, criteria proposed by previous workers suggest that the majority of flames investigated in this study are representative of wrinkled laminar flames. To establish this conclusion more concretely, a simple WLF model was used to predict the T' levels characteristic of WLF. These predictions and the experimental T' data were then used to examine the consistency between the model and the flame studied.

The flame model, based on the mechanistic WLF concept, assumes that the mean flame temperature profile measured in combustor-fixed coordinates results from spatial fluctuations of a laminar flame sheet. It is assumed that turbulence does not alter the laminar flame structure. Turbulence and flame propagation interact to result in flame motion. With an assumed laminar flame structure and flame sheet position probability density function (pdf) and a measured flame brush thickness, peak T' levels can be calculated.

The terminology employed is presented in Fig. 8. Two coordinate systems are defined. The coordiante system δ moves with the laminar flame sheet. The X coordinate system is fixed relative to the combustor. Each point in δ is characterized by a constant temperature. The points δ_c and δ_H are defined as the initial and final points of the laminar flame temperature profile in the δ system. δ_F, the laminar flame thickness, is equal to $(\delta_H - \delta_c)$. $T_f(\delta)$ is the local laminar flame temperature at any point δ.

Formally, the mean temperature at any point x' in the combustor-fixed coordinate system is

$$\bar{T}_{x'} = \int_{-\infty}^{\delta_C} T_0 P(\delta;x')\,d\delta + \int_{\delta_C}^{\delta_H} T_f(\delta) P(\delta;x')\,d\delta + \int_{\delta_H}^{\infty} T_b P(\delta;x')\,d\delta$$

where $P(\delta;x')d\delta$ represents the probability that a flame segment from δ to $\delta + d\delta$ is located at the point x'. Similarly

$$T'^2_{x'} = \int_{-\infty}^{\delta_C} (T_0 - \bar{T}_{x'})^2 P(\delta;x')\,d\delta + \int_{\delta_C}^{\delta_H} (T_f - \bar{T}_{x'})^2 P(\delta;x')\,d\delta + \int_{\delta_H}^{\infty} (T_b - \bar{T}_{x'})^2 P(\delta;x')\,d\delta \quad (1)$$

Both the laminar flame temperature profile, $T_f(\delta)$, and the statistical history of the flame motion about x' are required to predict T' at x'.

Although T_f and $P(\delta;x)$ are not available from this study, reasonable forms for these functions can be postulated to estimate T' levels characteristic of a WLF. Such an analysis was conducted to predict the maximum T' characterizing the flames experimentally investigated. The analysis employed the following assumptions:

1) $T_f(\delta)$ is a linear function:

$$T_f = T_0 \text{ for } \delta \le \delta_c$$
$$= T_b \text{ for } \delta \ge \delta_H$$
$$= T_0 + (\delta - \delta_c)(T_b - T_0/\delta_F) \text{ for } \delta_c < \delta < \delta_H$$

2) $\bar{T}(x)$, the time mean temperature profile measured in laboratory coordinates, is a linear function. The geometric center of the flame brush is defined as $\bar{x}$. X_{min} and X_{max} are the extremes of the flame brush.

3) $P(\delta;\bar{x})$ has a triangular shape, symmetric about the point $\bar{\delta}$ and with a maximum at $\bar{\delta}$. Therefore, $\bar{\delta}$ represents the geometric center of the fluctuating laminar flame sheet: $T_f(\bar{\delta}) = 0.5\,(T_b + T_0)$.

As has been demonstrated by Karlovitz, $P(\delta;\bar{x})$ is closely normal for flames purported to be WLF.[21] The adopted pdf was chosen for analytical convenience. With the assumed symmetry of this analysis, $\bar{x}$ represents the time mean position of $\bar{\delta}$ and $\bar{T}_{\bar{x}} = T_f(\bar{\delta})$. The assumed temperature profiles and pdf result in the model predicting maximum T' values at the point $\xi = \frac{1}{2}$.

$T'_{\bar{x}}$ values were predicted using experimentally measured mean temperature profiles. These profiles were used to determine time mean flame brush thicknesses at different locations in the flames. These flame brush thickness data are presented in Fig. 9. Flame thickness increases with increased approach flow turbulence intensity and with downstream distance from the flameholder.

The flame brush thickness for a particular combination of turbulence generator ϕ and vertical position was used to quantify $\bar{x}$, X_{min}, and X_{max}. A previously calculated value of

laminar flame thickness (calculation method to be described subsequently) was used to determine δ_c, δ_H, and $\bar{\delta}$. The function $T_f(\delta)$ could then be specified. With these quantities known, $\delta_{\min}$ and $\delta_{\max}$ could be calculated:

$$\delta_{\min} = \delta_H - (X_{\max} - \bar{x})$$

$$\delta_{\max} = \delta_c + (\bar{x} - X_{\min})$$

$\delta_{\min}$ and $\delta_{\max}$ represent the extreme points on the flame-fixed coordinate system that attain a position in space over $\bar{x}$. More specifically, when δ_H coincides with $X_{\max}$, $\delta_{\min}$ coincides with $\bar{x}$. Similarly, $\delta_{\max}$ coincides with $\bar{x}$ when δ_C is located at $X_{\min}$.

The quantities $\delta_{\min}$ and $\delta_{\max}$ allow the flame position pdf to be formulated, since

$$P(\delta_{\max};\bar{x}) = P(\delta_{\min};\bar{x}) = 0$$

and

$$\int_{\delta_{\min}}^{\delta_{\max}} P(\delta;\bar{x})\,\mathrm{d}\delta = 1$$

With $P(\delta;\bar{x})$ finally determined for a specific flame and vertical location, $T'_{\bar{x}}$ was then calculable using using Eq. (1).

For these $T'_{\bar{x}}$ calculations, an appropriate laminar flame thickness δ_F was required. A value of δ_F was chosen so as to properly predict the peak T' measured in the flame above the no. 20 mesh with $h = 4.8$ cm and $\phi = 0.85$. This value of δ_F was adopted for all cases where $\phi = 0.85$. For $\phi = 0.75$, δ_F was found from

$$\delta_{F_{\phi=0.75}} = \delta_{F_{\phi=0.85}} \left[\frac{S_{L_{\phi=0.85}}}{S_{L_{\phi=0.75}}} \right]$$

The predicted value of δ_F obtained by this method was 0.94 mm at $\phi = 0.85$. This flame thickness is of the same order of magnitude as laminar flame thickness values presented for typical hydrocarbon fuel-air flames at atmospheric pressure.[18]

The results of the $T'_{\bar{x}}$ predictions based on this WLF model can be summarized as follows:

1) The model does predict an increase in $T'_{\bar{x}}$ with height in any particular flame and with increasingly coarse turbulence generators. This behavior is associated with increases in the flame brush thickness with increased height and turbulence level.

2) The model predicts an increase in $T'_{\bar{x}}$ with ϕ more than is attributable to an increase in T_b with ϕ. This is due to the decrease in the laminar flame thickness with increased ϕ, resulting in a greater percentage of time during which extreme temperatures are experienced at $\bar{x}$.

3) The model predicts that the maximum T' should occur at $\xi = \frac{1}{2}$. Experimental results indicated that T' maximums for the no. 20 and no. 10 meshes generally occurred between $\xi = 0.4$ and 0.5. The grid generator showed a larger deviation from the predicted behavior. T' peaks occurred for $\xi < 0.4$.

4) The predicted T' values do not agree particularly well with the experimentally determined values. The model predictions range from 84% to approximately 400% of the measured values. The disagreement increases with increases in the measured flame brush thickness. Therefore, the disagreement increases with increased turbulence levels and height above the flameholder. Agreement is best for the no. 20 and no. 10 meshes. The predicted T' values for the grid generator flames are uniformly high, ranging from 300% to 400% of the measured values.

The qualitative agreement between the employed WLF model and the mildly turbulent flames above the no. 10 and no. 20 meshes tends to support the idea that these flames are most appropriately characterized as wrinkled laminar flames. However, the grid turbulence flames differ from the model by exhibiting T' peaks at ξ values significantly lower than 0.5. In addition, the grid turbulence flames show the largest disagreement with the predicted T' magnitudes. Therefore, it appears that these flames are representative of a more intensely turbulent combustion regime than the wrinkled laminar flame.

Conclusion

A number of turbulent flame speed correlations found in the literature were examined using the experimental data obtained in this study. Correlations involving S_t/S_L vs $Re_\ell^{1/2}$ and S_t/S_L vs Re_λ appeared equally successful. However, the former set of parameters is commonly associated with the mildly turbulent wrinkled laminar flame regime. The latter correlation was suggested for intensely turbulent flames. Clearly, although these relatively simple correlations are capable of indicating trends in flame speed behavior, they cannot, at present, be used to establish flame structure.

Based on comparisons of flame temperature fluctuation measurements and temperature fluctuation predictions using a wrinkled laminar flame model, it appears that two regimes of flame structure were represented by the flames investigated in this study. Good agreement between the model and flames in low-intensity turbulence indicates that these flames are wrinkled laminar flames. Poor agreement between the model and more intensely turbulent flames, particularly with regard to the location of the maximum temperature fluctuations, suggests that a wrinkled laminar flame structure is not appropriate for these flames. These conclusions tend to support simple criteria proposed by previous workers that indicate the conditions in which a wrinkled laminar flame structure is appropriate.

Acknowledgment

This research was supported by NASA Grant NSG 3019, C. J. Marek, Grant Monitor.

References

[1] Smith, K. O. and Gouldin, F. C., "Experimental Investigation of Flow Turbulence Effects on Premixed Methane-Air Flames," AIAA *Progress in Astronautics and Aeronautics—Turbulent Combustion*, Vol. 58, edited by L. A. Kennedy, New York, 1978, p. 37.

[2] Andrews, G. E. and Bradley, D., "Determination of Burning Velocities: A Critical Review," *Combustion and Flame*, Vol. 18, Feb. 1972, p. 133.

[3] Scadron, M. D. and Warshawsky, I., "Experimental Determination of Time Constants and Nusselt Numbers for Bare-Wire Thermocouples in High-Velocity Air Streams and Analytic Approximation of Conduction and Radiation Errors," NASA TN 2599, Jan. 1952.

[4] Smith, K. O., "Experimental Investigation of Flow Turbulence Effects on Premixed Methane-Air Flames," Ph.D. Thesis, Mechanical and Aerospace Engineering, Cornell University, Ithaca, N.Y., May 1978.

[5] Andrews, G. E., Bradley, D., and Lwakabamba, S. B., "Turbulence and Turbulent Flame Propagation—A Critical Appraisal," *Combustion and Flame*, Vol. 24, June 1975, p. 285.

[6] Libby, P. A. and Williams, F. A., "Turbulent Flows Involving Chemical Reactions," *Annual Review of Fluid Mechanics*, Vol. 8, 1976, p. 351.

[7] Ballal, D. R. and Lefebvre, A. H., "The Structure and Propagation of Turbulent Flames," *Proceedings of the Royal Society of London A*, Vol. 344, June 24, 1975, p. 217.

[8] Klimov, A. M., "Laminar Flame in a Turbulent Flow," *Journal of Applied Mechanics and Technical Physics*, Vol. 3, 1963, p. 49.

[9] Summerfield, M., Reiter, S. H., Kebely, V., and Mascolo, R. W., "The Structure and Propagation Mechanism of Turbulent Flames in High Speed Flow," *Jet Propulsion*, Vol. 25, Aug. 1955, p. 377.

[10] Schetinkov, E. S., "Calculation of Flame Propagation in a Turbulent Flow," *Combustion in Turbulent Flow*, edited by L. H. Khitrin, Israel Program for Scientific Translations, Jerusalem, 1963, p. 1.

[11] Chomiak, J., "Application of Chemiluminescence Measurement to the Study of Turbulent Flame Structure," *Combustion and Flame*, Vol. 18, June 1972, p. 429.

[12] Kovasnay, L.S.G., "Combustion in Turbulent Flow," *Jet Propulsion*, Vol. 26, June 1956, p. 485.

[13] Tennekes, H. and Lumley, J. L., *A First Course in Turbulence*, MIT Press, Cambridge, Mass., 1972.

[14] Andrews, G. E., Bradley, D., and Lwakabamba, S. B., "Measurement of Turbulent Burning Velocity for Large Turbulent Reynolds Numbers," *15th Symposium (International) on Combustion*, The Combustion Institute, 1975, p. 655.

[15] Gouldin, F. C., "Statistical Model for Premixed Turbulent Flames," The Combustion Institute Joint Meeting, San Antonio, Texas, April 21-22, 1975.

[16] Sanematsu, H. S., "Turbulent Flame Propagation in a Homogeneous Gas Mixture," *Combustion and Flame*, Vol. 13, Feb. 1969, p. 1.

[17] Wagner, P., "Burning Velocities of Various Premixed Turbulent Propane Flames on Open Burners," NACA TN 3575, 1955.

[18] Bradley, J. N., *Flame and Combustion Phenomena*, Methuen, London, 1969.

[19] Abdel-Gayed, R. G. and Bradley, D., "Dependence of Turbulent Burning Velocity on Turbulent Reynolds Number and Ratio of Laminar Burning Velocity to R.M.S. Turbulent Velocity," *16th Symposium (International) on Combustion*, Combustion Institute, 1976, p. 1725.

[20] Gouldin, F. C., "Model for Premixed Turbulent Flames," The Combustion Institute Spring Meeting, Cleveland, Ohio, March 28-30, 1970, 1977.

[21] Karlovitz, B., Denniston, D. W., Knapschaefer, D. H., and Wells, F. E., "Studies on Turbulent Flames," *4th Symposium (International) on Combustion*, The Combustion Institute, 1953, p. 613.